J Bioenerg Biomembr (2007) 39:275–289
DOI 10.1007/s10863-007-9089-7

ORIGINAL PAPER

# The boxing glove shape of subunit *d* of the yeast V-ATPase in solution and the importance of disulfide formation for folding of this protein

**Youg R. Thaker · Manfred Roessle · Gerhard Grüber**

Received: 27 April 2007 / Accepted: 15 May 2007 / Published online: 26 September 2007


**Abstract** The low resolution structure of subunit *d* (Vma6p) of the *Saccharomyces cerevisiae* V-ATPase was determined from solution X-ray scattering data. The protein is a boxing glove-shaped molecule consisting of two distinct domains, with a width of about 6.5 nm and 3.5 nm, respectively. To understand the importance of the N- and C-termini inside the protein, four truncated forms of subunit *d* ($d_{11–345}$, $d_{38–345}$, $d_{1–328}$ and $d_{1–298}$) and mutant subunit *d*, with a substitution of Cys329 against Ser, were expressed, and only $d_{11–345}$, containing all six cysteine residues was soluble. The structural properties of *d* depends strongly on the presence of a disulfide bond. Changes in response to disulfide formation have been studied by fluorescence- and CD spectroscopy, and biochemical approaches. Cysteins, involved in disulfide bridges, were analyzed by MALDI-TOF mass spectrometry. Finally, the solution structure of subunit *d* will be discussed in terms of the topological arrangement of the $V_1V_O$ ATPase.

**Keywords** Vacuolar-type ATPase · $V_1V_O$ ATPase · $V_1$ ATPase · Vma6p · Subunit *d* · Small angle X-ray scattering · $A_1A_O$ ATP synthase · Subunit C · Peripheral stalk

Y. R. Thaker · G. Grüber (✉)
School of Biological Sciences,
Nanyang Technological University,
60 Nanyang Drive,
Singapore 637551, Singapore
e-mail: ggrueber@ntu.edu.sg

M. Roessle
European Molecular Biology Laboratory, Hamburg Outstation,
EMBL c/o DESY,
22603 Hamburg, Germany

**Abbreviations**

| | |
|---|---|
| BSA | bovine serum albumin |
| CD | circular dichroism |
| DTT | Dithiothreitol |
| EDTA | ethylenediaminetetraacetic |
| EM | electron microscopy |
| IPTG | isopropyl-β-D-thio-galactoside |
| NEM | N-ethyl maleimide |
| NMR | nuclear magnetic resonance |
| NTA | nitrilotriacetic acid |
| PAGE | polyacrylamide gel electrophoresis |
| PCR | polymerase chain reaction |
| SAXS | small angle X-ray scattering |
| SDS | sodium dodecyl sulfate |
| TMR | tetramethyl rhodamine |
| Tris | Tris-(hydroxymethyl)aminomethane |

## Introduction

The proton-translocating vacuolar ATPase ($V_1V_O$ ATPase) is a multi-subunit complex common to all eukaryotic cells. This enzyme is found on the intracellular organelles of all eukaryotes and also on the plasma membrane of specialized cell types. ATP hydrolysis by the V-ATPases drives the transport of protons into the luminal of organelles, which this macromolecular complex decorates. As suggested by its bipartite name, the $V_1V_O$ ATPase is composed of a water-soluble $V_1$ ATPase and an integral membrane subcomplex, $V_O$ (Fig. 1). ATP is hydrolyzed on the $V_1$ headpiece consisting of an $A_3$:$B_3$ hexamer, and the energy released during that process is transmitted to the membrane-bound $V_O$ domain, to drive the ion translocation (Lolkema et al. 2003; Margolles-Clark et al. 1999) This energy-

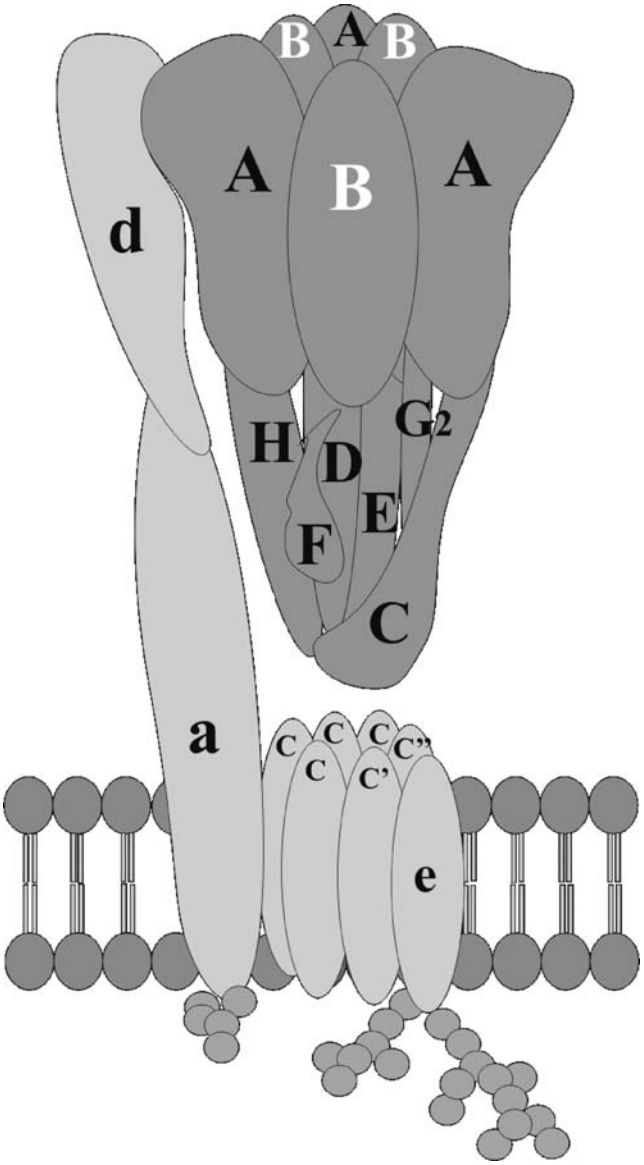


**Fig. 1** Schematic diagram of the $V_1$ (*dark gray*) and $V_O$ section (*gray*) of the eukaryotic vacuolar ATPase. In this type of V-ATPase the ATPase active $V_1$ part can be reversibly disconnected from the proton-translocating $V_O$ part (Wieczorek et al. 1999)

coupling occurs via the so-called "stalk" structure, an assembly of the $V_1$ and $V_O$ subunits C–H and *a* and *d*, respectively, that forms the functional and structural interface. The proposed subunit stoichiometry of $V_1$ is $A_3$:$B_3$:$C_1$:$D_1$:$E_1$:$F_1$:$G_2$:$H_x$ (Müller and Grüber 2003; Inoue et al. 2003). The integral $V_O$ domain contains five different subunits in a stoichiometry of $a_1$:$d_1$:$c_{4-5}$:$c_1'$:$c_1''$ (Inoue et al. 2003). The $V_O$ complex can be subdivided into two parts that rotate relative to each other, the peripheral stalk and the proton-translocating ring. The $V_O$ part of the stator is proposed to consist of subunit *a* (Venzke et al. 2005; Wilkens and Forgac 2001) and *d* (Clare et al. 2006). The proton-translocating ring is composed of the subunits $c_{4-5}$: $c_1'$:$c_1''$, each having multiple transmembrane domains and are termed proteolipids because of their hydrophobic nature (Clare et al. 2006). The fifth $V_O$ subunit, subunit *d*, is predicted to be a hydrophilic peripheral membrane protein (Bauerle et al. 1993). Its precise contribution to $H^+$–ATPase function is unclear, although it has been suggested that *d* might play a role in coupling ATP cleavage and proton transport (Nishi et al. 2003) and essential for embryonic development (Miura et al. 2003). The gene encoding subunit *d* of the yeast $V_1V_O$ ATPase was initially cloned as the *VMA6* gene, where its disruption was shown to lead to a typical Vma-phenotype (Bauerle et al. 1993). *Vma6p* has no transmembrane anchoring regions in its sequence (Bauerle et al. 1993), but has been found to remain firmly attached to the $V_O$ sector when $V_1$ part of the $V_1V_O$ ATPase is removed in vitro by treatment with chaotropic agents (Adachi et al. 1999) and also during in vivo disassembly of $V_1$ from $V_O$ upon glucose withdrawal (Kane 1995) subunit *d* remains associated with $V_O$ domain. These studies suggest that subunit *d* is attached to $V_O$ domain by protein–protein interactions rather than being directly anchored to membrane region. Its peripheral position is further supported by the fact that mild proteolysis results in rapid cleavage of subunit *d* in intact clathrin-coated vesicles (Zhang et al. 1992).

Here we have turned our attention to the examination of subunit *d* (Vma6p) from *Saccharomyces cerevisiae* V-ATPase and described the production and purification of subunit *d* and the analysis of its secondary and tertiary structure in solution using circular dichroism spectroscopy (CD) and small angle X-ray scattering (SAXS), respectively. Evidence is presented that formation of intramolecular disulfide bond is essential for proper folding and solubility of the protein.

## Experimental procedures

### Biochemicals

ProofStart™ DNA Polymerase and $Ni^{2+}$-NTA-chromatography resin were received from Qiagen (Hilden, Germany); restriction enzymes were purchased from Fermentas (St. Leon-Rot, Germany). The expression vector pET9d1-$His_3$ was provided by S. M. Bailer, (Universitätsklinikum Homburg/Saar, Germany). Yeast genomic DNA was kindly provided by Dr. T. Thanabalu (SBS/NTU, Singapore). Chemicals for gel electrophoresis were received from Serva (Heidelberg, Germany). Bovine serum albumin was purchased from GERBU Biochemicals (Heidelberg, Germany). All other chemicals were at least of analytical grade and received from BIOMOL (Hamburg, Germany), Merck (Darmstadt, Germany), Roth (Karlsruhe, Germany), Sigma (Deisenhofen, Germany), or Serva (Heidelberg, Germany).

## Constructs, mutagenesis and proteins

To amplify the *VMA6* coding region, oligonucleotide primers 5′-CATGCCATGGTAATGGAAGGCGTG-3′ (forward primer) and 5′-CGTTCGAGCTCTCAATAAACG GAAATATAATTG-3′ (reverse primer), incorporating *Nco*I and *Sac*I restriction sites, respectively (underlined), were designed. *S. cerevisiae* genomic DNA was used as template for the polymerase chain reaction (PCR). Following digestion with *Nco*I and *Sac*I, the PCR product was ligated into the pET9d1-$His_3$ vector. The pET9d1-$His_3$ vector containing the *VMA6* insert was then transformed into *E. coli* cells (strain Rosetta-gami 2 (DE3); Novagen) and grown on 30 μg/ml kanamycin, tetracycline (12.5 μg/ml) and chloramphenicol (35 μg/ml)-containing Luria-Bertoni (LB) agar-plates. To express $His_3$-Vma6p, liquid cultures were shaken in LB medium containing appropriate antibiotics for about 6 h at 30°C until an optical density $OD_{600}$ of 0.6–0.7 was reached. To induce expression of $His_3$-Vma6p, the cultures were supplemented with isopropyl-β-D-thio-galactoside (IPTG) to a final concentration of 1 mM. Following incubation for another 4 h at 30°C, the cells were harvested at 10,000×*g* for 15 min, 4°C. Subsequently, they were lysed on ice by sonication for 3×1 min at 50% power in buffer A (50 mM Tris/HCl, pH 7.5, 500 mM NaCl, 1 mM DTT and 4 mM Pefabloc SC (BIOMOL)). The lysate was cleared by centrifugation at 10,000×*g* for 30 min at 4°C, the supernatant was passed through a filter (0.45 μm pore-size) and supplemented with $Ni^{2+}$-NTA resin. The His-tagged protein was incubated with Ni NTA matrix for 3 h at 4°C and protein was eluted with an imidazole-gradient (25–200 mM) in buffer A by mixing on a sample rotator (Neolab). Fractions containing $His_3$-Vma6p/subunit *d* were identified by SDS-PAGE[1] (16), pooled and concentrated using Centriprep YM-30 (30 kDa molecular mass (MM) cut off) spin concentrators (Millipore) and subsequently applied on an ion-exchange column (Source™ 30Q, Amersham Biosciences). The protein was purified using a step gradient with buffer A (50 mM Tris/HCl (pH 7.5), 50 mM NaCl and 1 mM DTT) and Buffer B (50 mM Tris/HCl (pH 7.5), 1 M NaCl and 1 mM DTT). The purity of the protein sample was analyzed by SDS-PAGE (Laemmli 1970). The SDS-gels were stained with Coomassie Brilliant Blue R250. Protein concentrations were determined by the bicinchonic acid assay (BCA; Pierce, Rockford, IL. USA).

In order to obtain N-terminal truncated forms of subunit *d*, including only residues $d_{11–345}$ and $d_{38–345}$, primers 5′ CATG*CCATGG*TTACGTTGGAAGATC 3′ (forward primer), 5′-CGTTC*GAGCTC*TCAATAAACGGAAATA TAATTG-3′ (reverse primer) and 5′CATGCCATGG TAGGGTTTATTGAAGGTG3′ (forward primer), 5′-CGTTC*GAGCTC*TCAATAAACGGAAATATAATTG-3′ (reverse primer), were designed, respectively. In addition, C-terminal truncated forms of subunits *d*, $d_{1–328}$ and $d_{1–298}$ were amplified using primers sets: 5′-CATG*CCATGG* TAATGGAAGGCGTG-3′ (forward primer) and 5′ CGTC*GAGCTC*TCAATCTCTACATAGTTCC3′ (reverse primer), 5′-CATG*CCATGG*TAATGGAAGGCGTG-3′ (forward primer) and 5′ CGTC*GAGCTC*TCATTCAGCAATC CAG 3′ (reverse primer), respectively. In all constructs the restriction sites *Nco*I and *Sac*I were incorporated. Following digestion with *Nco*I and *Sac*I, the pair PCR products were ligated into the pET9d1-$His_3$ as described for the entire subunit *d*. Truncated subunits of *d* were purified with $Ni^{2+}$-NTA resin column, followed by ion-exchange purification using Resource Q column as described above for the entire subunit *d*.

The Cystein mutant of subunit *d* (Vma6p) C329S was cloned using forward primer 5′ CATG*CCATGG*TAATG GAAGGCGTGTATTTCAACATTGACAATG 3′ and reverse primer 5′ TTC*GAGCTC*TCAATAAACGGAAATA TAATTGTTGATTCTTTCTCTTTGATTTTGTGC TATTGA 3′ for PCR amplification from yeast genomic DNA. The amplified PCR product was digested with *Nco*I and *Sac*I enzymes and ligated into pET9d1-$His_3$ vector. C329S substitution was further confirmed by sequencing. The pET9d1-$His_3$ vector, containing the gene *VMA6 C329S*, was then transformed into *E. coli* cells (strain Rosetta-gami 2 (DE3)) and grown on kanamycin/tetracycline/chloramphenicol-containing Luria-Bertoni (LB) agar-plates. To express $His_3$-Vma6p C329S mutant, liquid cultures were shaken in LB medium containing kanamycin/tetracycline/chloramphenicol as described above for other constructs.

## One dimensional $^1H$ NMR spectroscopy

A solution containing subunit *d* at a concentration of 230 μM was prepared in an aqueous buffer containing phosphate buffer, 50 mM NaCl, at pH 6.5 and 10% $D_2O$ (*v*/*v*). The NMR spectra were collected at 288 K on an Avance600 spectrometer (Bruker, Billerica, MA). The spectra were processed and analyzed with the program ZGGPW5 (Bruker, (17)).

## Determination of native molecular mass

Gel filtration chromatography was performed using a Superdex 75 HR 10/30 column (Amersham Biotech) using a buffer of 50 mM Tris/HCl (pH 7.5) and 370 mM NaCl. To construct a calibration curve, a set of standard proteins (Amersham Biotech and Sigma) was analyzed. The $K_{av}$ parameter was determined ($K_{av}=(V_e-V_0)/(V_t-V_0)$, where $V_e$ represents the elution volume, $V_0$ the void volume, and $V_t$ the total bed volume). The $K_{av}$ values for standard proteins were plotted as a function of the logarithm of molecular

mass, and the resulting calibration curve was used to derive the molecular mass of Vma6p (subunit *d*).

## CD spectroscopy

Steady state CD spectra were measured in the far UV-light (190–260 nm) using a CHIRASCAN spectropolarimeter (Applied Photophysics). Spectra were collected in a 60 µl quartz cell (Hellma) at 18°C at a step resolution of 1 nm. To remove DTT from the buffer used for protein isolation, subunit *d* was dialyzed in a QuixSep™ Micro Dialyzer (Roth, Germany) for 6 h against degassed buffer containing 50 mM Tris/HCl, pH 7.5, and 340 mM NaCl using a 10 kDa Spectra/Por dialysis membrane (Spectrum Laboratories, Canada). CD spectroscopy of subunit *d* (2.0 mg/ml) was performed in 50 mM Tris/HCl, pH 7.5, and 340 mM NaCl in the absence and presence of 1 mM DTT, respectively. The spectrum for the buffer was subtracted from the spectrum of subunit *d*. This baseline corrected spectrum was used as input for computer methods to obtain predictions of secondary structure.

## X-ray scattering experiments and data analysis of Vma6p (subunit d)

The synchrotron radiation X-ray scattering data were collected following standard procedures on the X33 beam line (Boulin et al. 1986, 1988) of the EMBL Hamburg on the storage ring DORIS III of the Deutsches Elektronen Synchrotron (DESY) using a MAR345 image plate with online readout (MarResearch, Norderstedt, Germany). The scattering patterns from subunit *d* at protein concentrations of 0.8, and 12.7 mg/ml were measured using a sample–detector distances of 2.4 m, covering the range of momentum transfer $0.1<s<4.5$ nm$^{-1}$ ($s=4\pi \sin(\theta)/\lambda$, where $\theta$ is the scattering angle and $\lambda=0.15$ nm is the X-ray wavelength). A sample volume of 60 µl was disposed in a small cuvette (1 mm thickness) with thin polystyrene windows (20 µm) and two repetitive measurements of 120 s of the same protein solution were performed in order to check for radiation damage. No aggregation was found during the initial 120 s exposure. The data were normalized to the intensity of the incident beam; the scattering of the buffer was subtracted and the different curves were scaled for concentration. All the data processing steps were performed using the program package PRIMUS (Konarev et al. 2003). The forward scattering $I(0)$ and the radius of gyration $R_g$ were evaluated using the Guinier approximation (Guinier and Fournet 1955) assuming that at very small angles ($s<1.3/R_g$) the intensity is represented by $I(s)=I(0)\exp(-(sR_g)^2/3)$. These parameters were also computed from the entire scattering patterns using the indirect transform package GNOM (Svergun 1993), which also provide the distance distribution function $p(r)$ of the particle. The molecular mass of subunit *d* was calculated by comparison with the forward scattering from the reference solution of bovine serum albumin (BSA[1]).

Low resolution models of the *d* subunit were built using two ab initio methods. The program DAMMIN (Svergun 1992, 1997) represents the protein shape as an ensemble of $M \gg 1$ densely packed beads inside a search volume (a sphere of diameter $D_{max}$). Each bead belongs either to the protein (index=1) or to the solvent (index=0), and the shape is thus described by a binary string of length *M*. Starting from a random string, simulated annealing (Svergun 1992) is employed to find a compact configuration of beads minimising the discrepancy $\chi$ between the experimental $I_{exp}(s)$ and the calculated $I_{calc}(s)$ curves:

$$\chi^2 = \frac{1}{N-1}\sum_j \left[\frac{I_{exp}(s_j) - cI_{calc}(s_j)}{\sigma(s_j)}\right]^2$$

where *N* is the number of experimental points, *c* is a scaling factor and $\sigma(s_j)$ is the experimental error at the momentum transfer $s_j$.

In a more versatile ab initio approach implemented in the program GASBOR (Svergun et al. 2001), the protein is represented as a collection of dummy residues (DR). Starting from randomly positioned residues, a chain-compatible spatial distribution of DR's inside the search volume is found by simulated annealing. The DR method permits an enhanced resolution, but the number of residues must be known a priori. For the subunit *d* ten GASBOR reconstructions were performed using 350 amino acid residues. These ten independent models were analyzed using the programs DAMAVER (Svergun et al. 2001) and SUBCOMB (Svergun et al. 2001). These packages align all possible pairs of models and identify the most probable model giving the smallest average discrepancy with the rest. An averaged model is computed by aligning all other models with the most probable one, computing the density map of beads and drawing the threshold corresponding to the excluded particle volume. The DAMMIN and the GASBOR approach resulted in similar models and the averaged DR model was used for further interpretations.

In order to compare the experimental data of subunit *d* with the atomic structure of the stalk subunit C of the $A_1A_O$ ATP synthase from *T. thermophilus*, the SAXS parameters of the high resolution model of subunit C (PDB entry 1r5z, (Bernstein et al. 1977), were extracted from its structure using the program CRYSOL (Svergun et al. 1995).

## Tryptophan fluorescence measurements

A *Varian Cary Eclipse* spectrofluorimeter was used, and all experiments were carried out at 20°C. The samples were

excited at 295 nm, and the emission was recorded from 310 to 380 nm with excitation and emission bandpasses set to 5 nm.

### Disulfide formation due to $CuCl_2$-treatment

In order to remove DTT, subunit *d* was dialyzed against degassed buffer containing 50 mM Tris/HCl, pH 7.5, and 340 mM NaCl using a 10 kDa Spectra/Por dialysis membrane as described above. Afterwards the protein was supplemented with 100 μM of $CuCl_2$ as a zero length crosslinker for 30 min on a sample rotator at 4°C. The reaction was stopped by addition of 1 mM EDTA. In the case of tetramethyl rhodamine (TMR) or N-ethyl maleimide (NEM) labeling, the non-reduced protein was supplemented with 30 μM of TMR or NEM for 30 min in buffer containing 50 mM Tris/HCl, pH 7.5, and 340 mM NaCl at 4°C. Samples were dissolved in DTT-free dissociation buffer, and applied to an SDS-polyacrylamide gel.

### Tryptic digest and MALDI-TOF analysis

The band of subunit *d* treated with $CuCl_2$, DTT and TMR (see above), respectively, was cut from the gel and destained overnight with a solution of 50 mM ammonium bicarbonate, 40% ethanol. The protein was digested in gel with trypsin (Promega) according to Roos et al. (1998) except that the bands had been washed three times with acetonitrile before drying them in a speed vacuum concentrator. Digested samples were desalted with a C18ZipTip (Millipore) and eluted with CHCA- (10 mg/ml α-cyano-4-hydroxycinnamic acid in 50% acetonitrile, 0.1% trifluoroacetic acid) or FA- (8 mg/ml 3-methoxy-4-hydroxycinnamic acid in 50% acetonitrile, 0.1% trifluoroacetic acid) matrix solution. 1–2 μl of matrix-analyte solution was spotted onto the MALDI plate and allowed to dry (29). Peptide mass mapping was performed by matrix assisted laser desorption-ionisation/time-of-flight mass spectrometry (MALDI-TOF MS) using a Voyager-DE STR Biospectrometry Workstation). The peptide map was acquired in reflectron positive-ion mode with delayed extraction at a mass range of 900–8,000 Da. The instrument was calibrated using a calibration mixture (Applied Biosystems). For interpretation of the protein fragments, the PEPTIDEMASS (Wilkins et al. 1997) program available at Expasy web site (www.expasy.ch/tools/peptide-mass.html) was used.

## Results

### Purification of subunit d (Vma6p)

Induction of recombinant protein expression under the conditions specified in "Experimental procedures" resulted in production of an approximately 41 kDa protein which was found entirely within the soluble fraction. A $Ni^{2+}$-NTA resin column and an imidazole-gradient (25–200 μM) was used to separate $His_3$-Vma6p/subunit *d* from the main contaminating proteins. The recombinant protein eluted at 100 mM imidazole, was collected and subsequently applied to a RESOURCE™ Q column. Subunit *d* containing fractions were found in one distinct peak at approximately 340 mM of NaCl (Fig. 2). Analysis of the isolated protein by SDS-PAGE (Fig. 2) and MALDI mass spectrometry revealed the high purity of this protein, and confirmed the sequence-based predicted mass of 40.6 kDa, including the $His_3$-tag.

### Physical characterization of subunit d (Vma6p)

The purified protein was screened using 1D $^1H$ NMR spectroscopy to check their folded state. 1D $^1H$ NMR spectra of subunit *d* showed the characteristics of properly folded proteins featuring good dispersion of resonance lines amide protons (6 to 10 ppm), α-protons (3.5 to 5 ppm), and methyl protons (−0.5 to 1.0 ppm; Page et al. 2005; Fig. 3a).

The secondary structure of this subunit was determined from circular dichroism spectra, measured between 190–260 nm (Fig. 3b). The minima at 222 and 208 nm and the maximum at 192 nm indicate the presence of α-helical structures in the protein. Two computer based methods were used to analyze the CD spectrum of subunit *d*. The average secondary structure content was 58% α-helix and 36% random coil. This result is consistent with secondary structure predictions based on subunit *d* amino-acid

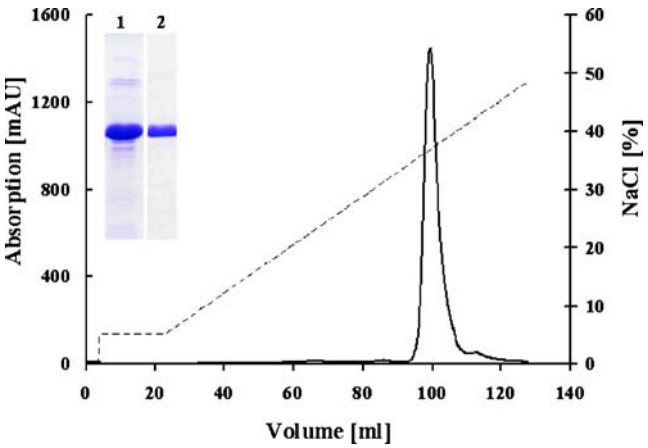


**Fig. 2** Chromatographic purification of *S. cerevisiae* subunit *d* (Vma6p). Following purification of the recombinant *d* on $Ni^{2+}$-NTA resin, the protein sample was applied onto a RESOURCE™ Q column (40 ml). After sample injection, an isocratic elution of five column volumes with buffer A [50 mM Tris/HCl (pH 7.5), 50 mM NaCl] and a flow rate of 6 ml/min was employed, followed by a gradient program 0 to 100% buffer B [Tris/HCl, pH 7.5, 1 M NaCl; (- - -)]. Twenty microliters each of the 100 mM $Ni^{2+}$-NTA fraction (*lane 1*) and ion-exchange purified main peak (*lane 2*) was applied on a 17.5% total acrylamide and 0.4% cross-linked acrylamide gel and stained with Coomassie Blue G250 (*insert*)

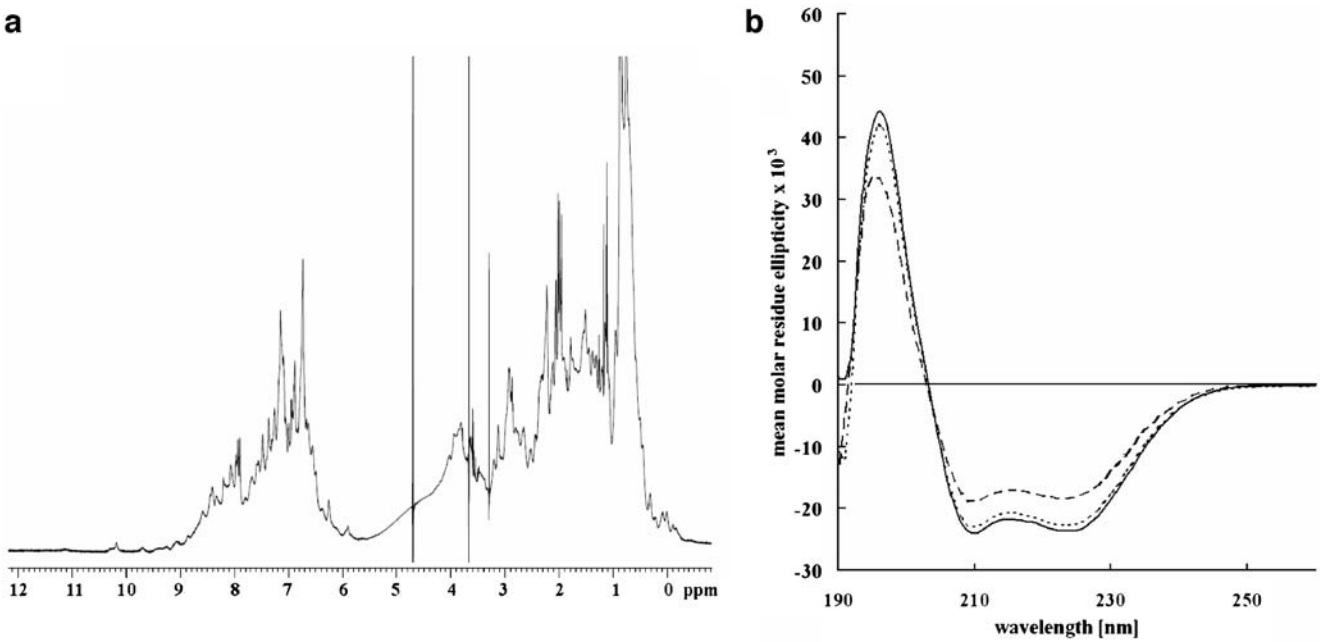


**Fig. 3** One-dimensional $^1$H NMR spectrum (**a**) and far UV-CD spectrum (**b**) of subunit *d* of the V-ATPase from yeast. **b** Subunit *d* in the presence (··) and absence (—) of DTT and the protein after $CuCl_2$-treatment (- -)

sequence. The molar ellipticity value at 208 nm and at 222 nm are 23,621.5 deg·cm$^2$·dmol$^{-1}$ and 23,658.3 deg·cm$^2$·dmol$^{-1}$, respectively, in a ratio of about 1.0. Since non-interacting helices typically give ratios of around 0.8, whereby interacting ones have ratios close to 1.0 (Burkhard et al. 2001), the CD spectrum presented indicates, that many of the residues in subunit *d* are in interactions.

## Determination of molecular mass and overall dimensions of the native d subunit

In order to determine the native molecular mass of subunit *d* (Vma6p), a Superdex 75 gel filtration column was calibrated by determining the $K_{av}$ values for a set of standard proteins of known molecular mass. A calibration curve based on these $K_{av}$ values is shown in Fig. 4b. Comparison of the $K_{av}$ for *d* versus the standards suggests the native molecular mass of approximately 47 ± 3 kDa. In a complementary approach, SAXS patterns from solutions of subunit *d* were recorded and processed as described in "Experimental procedures" to yield the final composite scattering curve in Fig. 5a. The initial portion of the scattering curve in the Guinier presentation is well approximated by a straight line (insert Fig. 5a), suggesting that the protein is monodisperse. The radius of gyration $R_g$ and the maximum dimension $D_{max}$ of subunit *d* are 2.74 ± 0.01 nm and 11 nm, respectively, suggesting that *d* is an elongated particle. Comparison with the scattering from the reference solutions of bovine serum albumin (BSA) yields the estimate of molecular mass of 46±4 kDa, in agreement with the results of the gel filtration chromatography and indicating that subunit *d* is monomeric at the concentrations used. Qualitative analysis of the distance distribution function suggests that *d* consists of a major part yielding a principal maximum in the $p(r)$ at around 3.1 nm (Fig. 5b) whereas the separated protuberance domain giving rise to a shoulder from 6.5 nm to 11±0.2 nm.

## Shape and domain structure of subunit d (Vma6p)

The gross structure of subunit *d* was restored ab initio from the scattering pattern in Fig. 5a using the shape determination program DAMMIN and the dummy residues modeling program GASBOR as described in "Experimental procedures". The two approaches yielded similar results. In the following, the models obtained with GASBOR are presented, which yield good fits to the experimental data in the entire scattering range (a typical fit displayed in Fig. 5a with a discrepancy $\chi$=2.32). Ten independent reconstructions yielded reproducible structure which is displayed in Fig. 6. Subunit *d* appears as a boxing glove-shaped molecule with two distinct domains. The major domain has dimensions of about 6.5×5.0 nm, and in the side view 6.5×4.5 nm, whereby the protuberance is about 3.5 nm in length and 2.0 nm in width.

## Disulfide bond formation(s) in subunit d

Subunit *d* from *S. cerevisiae* contains six cysteine residues three of which ($Cys_{36,127,329}$) are conserved in *d* subunits of

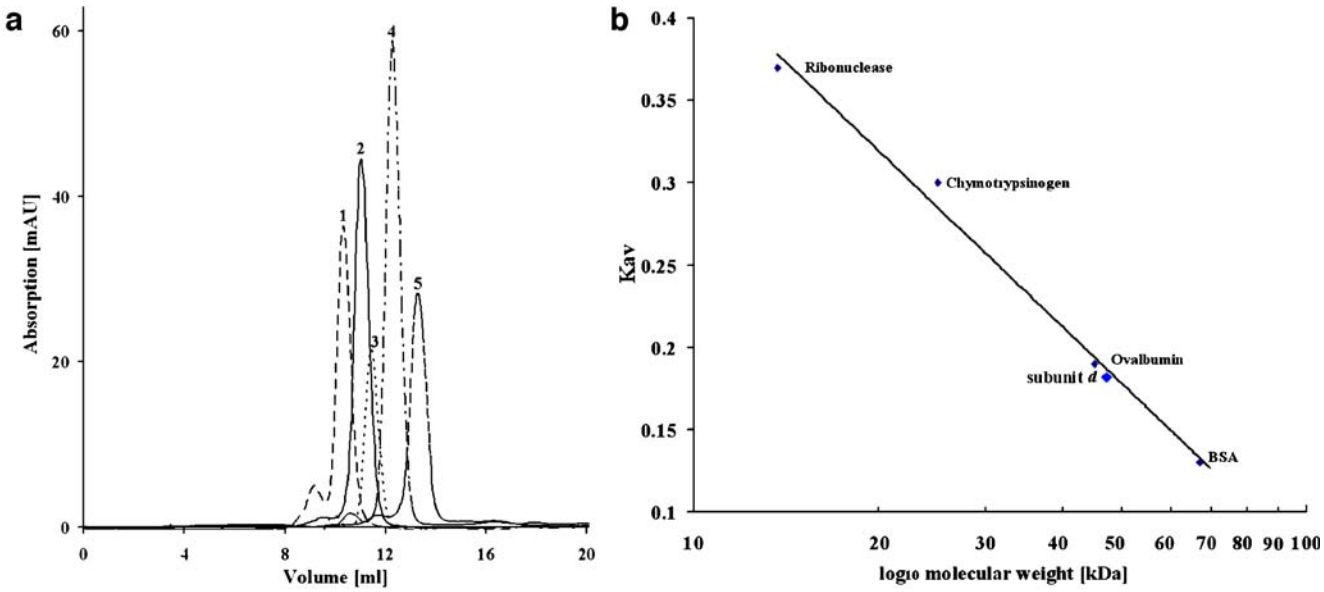


**Fig. 4** Determination of native molecular mass by gel filtration analysis. **a** The gel filtration analysis (Superdex 75 10/30 column) of subunit *d* (*peak 2*) was performed as described under "Experimental procedures". Proteins used as molecular size standards (*filled diamonds*) were BSA (67 kDa; *peak 1*), ovalbumin (45 kDa; *peak 3*), β-chymotrypsinogen A (25 kDa, *peak 4*) and ribonuclease A (13.7 kDa; *peak 5*). **b** For each protein, a *Kav* parameter was derived as described under "Experimental procedures". The *Kav* for subunit *d* is indicated

all eukaryotic V-ATPases described so far (Fig. 7). To explore a possible formation of disulfide bridges, the reduced and oxidized form of *d* were investigated by gel electrophoresis, in which disulfide bond-containing proteins migrate faster than their reduced counterparts, because the form containing disulfide is more compact (Svergun et al. 2000). When applied onto a polyacrylamide gel (Fig. 8a), the non-reduced form of subunit *d* (lane 1) migrates as a diffuse band. By comparison, upon reduction by dithiothreitol (DTT), the dithiol form of the protein migrates as a defined band (lane 3). When subunit *d* was supplemented with $CuCl_2$, to induce zero-length cross-link, the protein migrates further to the anode (lane 2). Upon reduction by DTT (lane 4), its mobility correspond to that of the reduced form of *d*. Since the mobility of the reduced subunit *d* is retarded, compared to the mobility of the $Cu^{2+}$-treated protein, the dithiol formation must lead either to a larger hydrodynamic volume or a lower net negative charge. In order to label accessible Cys residues inside *d*, the non-reduced form has been marked by tetramethyl rhodamine (TMR) with an additional mass of 486.91 Da, before SDS gel electrophoresis (Fig. 8b). The bands of the TMR-

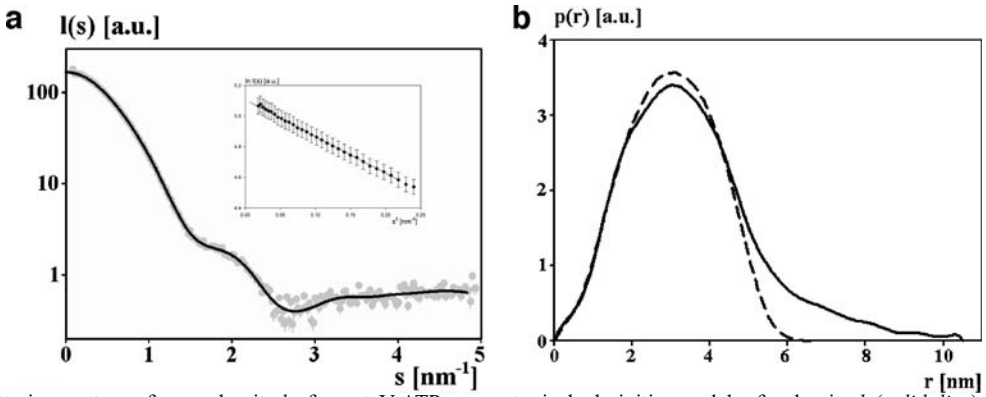


**Fig. 5** X-ray scattering patterns from subunit *d* of yeast V-ATPase. The *d* subunit at concentrations of 0.8, and 12.7 mg/ml, dissolved in 50 mM Tris/HCl (pH 7.5), 340 mM NaCl and 1 mM DTT, was measured using a detector to sample distances of 2.4 m. **a** Experimental SAXS curve from subunit *d* (*filled circles with error bars*); scattering from typical ab initio model of subunit *d* (*solid line*) computed by the program GASBOR (25). The Guinier plot with linear fit is shown in the *insert*. **b** Distance distribution functions of subunit *d* (*solid line*) and the high resolution structure of subunit C of the *T. thermophilus* $A_1A_O$ ATP synthase (pdb 1r5z; *dashed line*), respectively

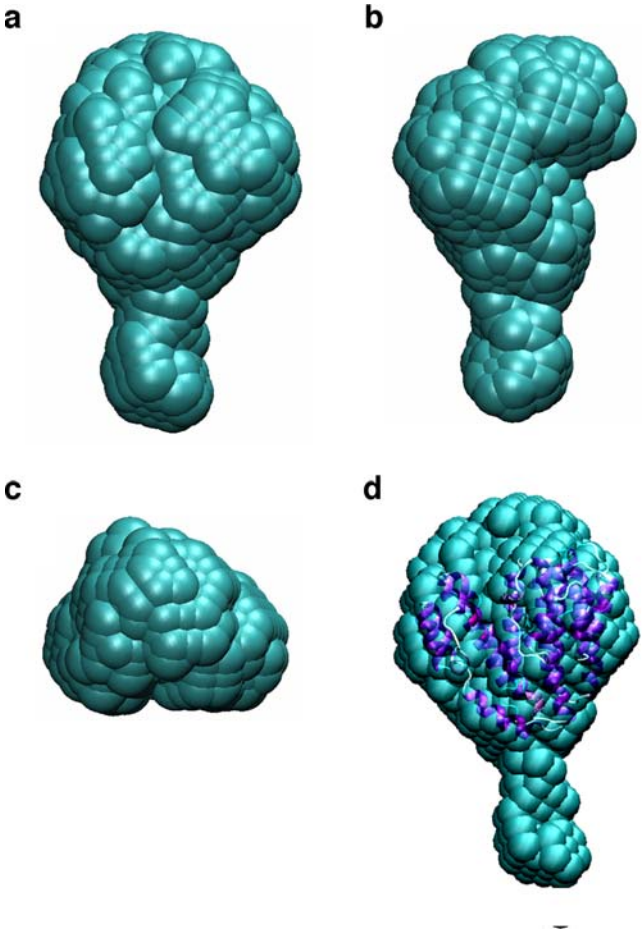


**Fig. 6** Low resolution structure of *d* of the yeast $V_1V_O$ ATPase in solution (**a**). The structures in the *middle* and *right panel* are rotated by 90° around the *y*- (**b**) and *x*-axis (**c**). **d** Superposition of the side-view of the low-resolution structure of subunit *d* with the C subunit of the $A_1A_O$ ATP synthase from *T. thermophilus* (pdb 1r5z)

labeled subunit *d*, and $Cu^{2+}$- and DTT-treated protein, respectively, were cut out for in-gel tryptic digestion and MALDI-TOF analysis. Using a variety of available software packages for mass fingerprinting, we identified 32 peptides covering 72% of the subunit *d* sequence. As summarized for proteins larger than 900 Da in Table 1 the four TMR-labeled proteins $_{164}$NCFDTAEELDDM NIEIIR$_{181}$, $_{206}$ECMQTLLGFEADR$_{218}$, $_{206}$ECMQTLLG FEADRR$_{219}$ and $_{277}$GFLETGNLEDHFYQLEMELCR$_{297}$ could be determined, indicating that the Cys residues 165, 207 and 296 are accessible in the protein. No bound fluorophor could be detected in the peptide $_{121}$GEIL QRCHPLGWFDTLPTLSVATDLESLYETVLVDTPLAP YFK$_{163}$. A mass of 4412.96 Da was found and an unequivocal identified as a crosslink product, occurring via the peptides $_{19}$GYRNGLLSNNQYINLTQCDTLELK$_{43}$ and $_{322}$NITWIAECIAQNQR$_{335}$, including the Cys$_{36}$ and Cys$_{329}$. When *d* was supplemented with $Cu^{2+}$ as a zero-length crosslinker an additional tryptic fragment of 6971.90 Da was generated, which is formed by the disulfide bridge of the two Cys residues 127 and 165 of the peptide $_{121}$GEIL QRCHPLGWFDTLPTLSVATDLESLYETVLVDTPLA PYFKNCFDTAEELDDMNIEIIR$_{181}$. By comparison, no crosslink product but smaller fragments of the N- and C-terminal part of *d* occured in the presence of the reducing agent DTT.

To exclude the possibility that Cys$_{36,\ 127,\ 329}$ might not have been labeled in the TMR-treated protein because of their inaccessibility to the TMR molecule or disulfide crosslink formation during the preparation of the digests for MALDI-TOF experiment, subunit *d* in the absence of DTT was labeled with the small alkylating agent N-ethyl maleimide (NEM (125.13 Da); see Experimental procedures), which has been successfully used for characterization of disulfide bond formation in protein folding studies (Mezghrani et al. 2001). As shown in Table 1 similar peptides of the trypsin cleaved, NEM-labeled *d* could be determined compared to the TMR marked subunit, including the peptides $_{19}$GYRNGLLSNNQYINLTQCDTLELK$_{43}$ and $_{322}$NITWIAECIAQNQR$_{335}$. The main difference between the NEM- and TMR labeled protein is given by the detection of the NEM labeled residue Cys$_{127}$, which became accessible for the smaller maleimide, NEM.

## Spectroscopic investigations

Subunit *d* contains four tryptophan residues, one at the N-terminus (Trp$_{132}$), and the other at the positions Trp$_{311,313,326}$. To obtain additional information on the structural properties of the reduced, nonreduced and $Cu^{2+}$-treated protein, the fluorescence emission of these states were monitored using the intrinsic fluorescence. The emission maximum of *d* is 337 nm (Fig. 9). Addition of DTT causes the quantum yield to increase, without noticeable shift in the spectrum. For comparison, addition of $CuCl_2$ to the protein caused the signal to decrease markedly and to shift the maximum to 341 nm, reflecting an intermediate polarity of the environment. The three states have also been studied by CD-spectroscopy. As demonstrated in Fig. 3b there is only a slight difference in the CD spectra of the non- and the reduced subunit *d*, which significantly alters when the protein is supplemented with $Cu^{2+}$. By comparison the $\Theta_{222}/\Theta_{208}$ ratio of the reduced and Cu-treated protein is 0.99 and 0.97, respectively. In order to determine whether the secondary structural alterations of the reduced and non-reduced subunit *d* were accompanied by changes of the tertiary structure of the protein, subunit *d* was investigated further by SAXS. The scattering curves (not shown) nearly coincide indicating that the tertiary structure of the non-reduced form does not diverge from that of the reduced subunit *d*.

```
                          1                                                  50
 S.cerevisiae     (1) ---------MEGVYFNIDNGFIEGVVRGYRNGLLSNNQYINLTQ DTLED
D. discoideum     (1) MGLFGGRKHGGLFTFNKDDGYLEAILRGFKKGILSRADYNNLCQ DNLED
     M. sexta     (1) ---------MKGCIFNIDAGYLEGLCRGFKCGILKQSDYLNLVQ ETLED
    N. crassa     (1) ---------MEGLLFNVNNGYIEGIVRGYRNSLLTSTNYTNMTQ ESIDD
    Consensus     (1)          MEGLIFNIDNGYIEGIVRGFKNGILSNSDYINLTQCDTLED
                          51                                                 100
 S.cerevisiae    (42) LKLQLSSTDYGNFLSSVSSESLTTSLIQEYASSKLYHEFNYIRDQSSGST
D. discoideum    (51) MKMHFISTDYGDFLAGEPSP-IHTTTIAEKATGKLVSEFNHIRNQAVEPL
     M. sexta    (42) LKLHLQGTDYGTFLANEPSP-LSVSTIDDKLREKLVIEFQHLRNHSVEPL
    N. crassa    (42) LKLQLG-PAYGDFLASLPPK-PSTSALAAKTTDKLVSEFRYVRANAAGSL
    Consensus    (51) LKLQL STDYGDFLASEPSP LSTSTIAEKATDKLVSEFNHIRNQAVGSL
                         101                                                 150
 S.cerevisiae    (92) RKFMDYITYGYMIDNVALMITGTIHDRDKGEILQR HPLGWFDTLPTLSV
D. discoideum   (100) STFMDFISYGYMIDNVVLLITGTLHERDISELVDK HPLGLFKSMATLSV
     M. sexta    (91) STFLDFITYSYMIDNIILLITGTLHQRPISELIPK HPLGSFEQMEAIHV
    N. crassa    (90) AKFMDYLTYGYMIDNVALLITGTLHERDTRELLER HPLGWFETMPVLCV
    Consensus   (101) STFMDFITYGYMIDNVALLITGTLHERDISELLDKCHPLGWFETMPTLSV
                         151                                                 200
 S.cerevisiae   (142) ATDLESLYETVLVDTPLAPYFKNCFDTAEELDDMNIEIIRNKLYKAYLED
D. discoideum   (150) VHNVADLYNNVLIDTPLAPYIQGCLS-EEDLDEMNNEIIRNTLYKAYLED
     M. sexta   (141) AATPAELYNAVLVDTPLAPFFVDCIS-EQDLDEMNIEIIRNTLYKAYLEA
    N. crassa   (140) ATNIEELYNSVMIETPLAPYFKSSLS-LQDLDELNIEIVRNTLYKNYLED
    Consensus   (151) ATNIEELYNSVLIDTPLAPYFK CLS EQDLDEMNIEIIRNTLYKAYLED
                         201                                                 250
 S.cerevisiae   (192) FYNFVT---EEIPEPAKECMQTLLGFEADRRSINIALNSLQSSDIDPDLK
D. discoideum   (199) FYNYCK----YLGGQTELIMSDILKFEADRRSINITINSFGATELSKDDR
     M. sexta   (190) FYDFCK----QIGGTTADVMCEILAFEADRRAIIITINSFG-TELSKDDR
    N. crassa   (189) FYHFVNTHPDMAGTPTAEVMSELLEFEADRRAINITLNSFG-TELSKADR
    Consensus   (201) FYNFVK   D IGGPTAEVMSEILAFEADRRAINITINSFGATELSKDDR
                         251                                                 300
 S.cerevisiae   (239) SDLLPNIGKLYPLATFHLAQAQDFEGVRAALANVYEYRGFLETG------
D. discoideum   (245) EKLYPSLGLLYPEGTSKLGKAEDVDQVRGILEVYSTYRNFFSDGVNNE--
     M. sexta   (235) AKLYPRCGKLNPDGLAALARADDYEQVKAVAEYYAEYSALFEGAGNNVGD
    N. crassa   (238) KKLYPNFGQLYPEGTLMLSRADDFEGVRLAVEGVADYKSFFDAAGLGGGP
    Consensus   (251) AKLYPNIGKLYPEGTA LARADDFEQVRAALE YAEYRAFFEAAGNN G
                         301                                                 350
 S.cerevisiae   (283) --------------NLEDHFYQLEMELCRDAFTQQFAISTVWAWMKSKEQ
D. discoideum   (293) -------------KSLEDSFFEHEVHLNRMAFEDQYGYGVFYAYIKLREQ
     M. sexta   (285) -------------KTLEDKFFEHEVNLNVHAFLQQFHFGVFYSYLKLKEQ
    N. crassa   (288) SGPGNMGGGGTEGKSLEDMFYQKEMEISKMAFTRQFTYAIVYAWVKLREQ
    Consensus   (301)               KSLED FFQHEMELNRMAFTQQFAYGVVYAWIKLKEQ
                         351                    377
 S.cerevisiae   (319) EVRNITWIAE IAQNQRERINNYISVY
D. discoideum   (330) EIRNIVWIAE ISQNMKQKMNQYIPIF
     M. sexta   (322) ECRNIVWISE VAQKHRAKIDNYIPIF
    N. crassa   (338) EIRNITWIAE IAQNQKERINNYISVF
    Consensus   (351) EIRNIVWIAECIAQNQKEKINNYISIF
```

**Fig. 7** Sequence alignment of V-ATPase *d* subunits from yeast (Bauerle et al. 1993), *Dictyostelium discoideum* (Temesvari et al. 1994), *Manduca sexta* (Merzendorfer et al. 1997) and *Neurospora crassa* (Melnik and Bowman 1996). Conserved cysteine residues are *boxed in blue*. Cysteins only found in *d* of the yeast V-ATPase are *highlighted in green*. Alignment was generated using AlignX (Vector NTI v9 InforMax)

## Traits of the N- and C-terminal truncated form of subunit d and the mutant C329S

In order to find out whether the N- and/or C-terminus of subunit *d*, including the residues $Cys_{36}$ and $Cys_{329}$, is/are involved in structure formation, four truncated forms of subunit *d* ($d_{11–345}$, $d_{38–345}$, $d_{1–328}$ and $d_{1–298}$) were constructed. The lack of 37 ($d_{38–345}$) and 17 ($d_{1–328}$), and 47 ($d_{1–298}$) residues at the N- and C-terminus, respectively, resulted in a low production of protein, which was insoluble. In contrast, expression of the truncated $d_{11–345}$ was similar in rate and solubility to wild type *d*. Consequently the $d_{11–345}$ protein was purified by metal chelate affinity chromatography and ion-exchange chromatography. Analysis of the isolated protein by MALDI mass spectrometry revealed a mass of 36 345 Da. The purified $d_{11–345}$ has been studied by CD-spectroscopy (Fig. 10a), indicating an α-helical content of 62% and 30% random coil and a $\Theta_{222}/\Theta_{208}$ ratio of 0.99. Incubation of $d_{11–345}$ in the presence of DTT or $CuCl_2$ and subsequent SDS-PAGE, resulted in the same migration pattern as described for the full-length protein in Fig. 8 (data not shown). To further substantiate the importance of the $Cys_{36}$ and $Cys_{329}$ for protein folding of subunit *d* the residue $Cys_{329}$ was substituted by a Ser residue in the mutant *d*C329S. SDS-PAGE and Coomassie staining revealed a prominent band

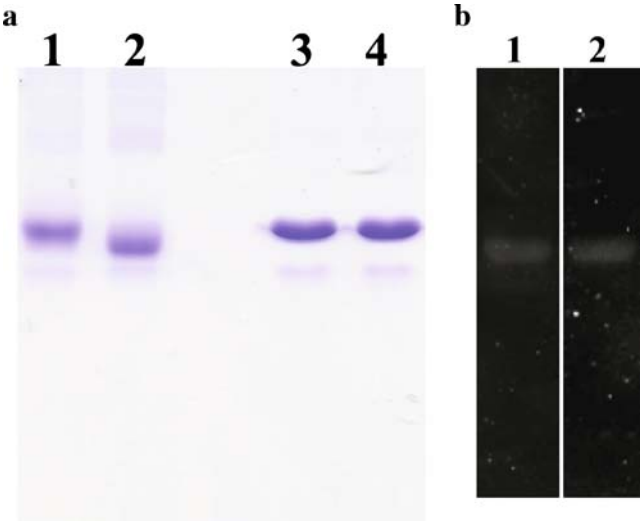


**Fig. 8** Electrophoretic analysis of the oxidized and reduced form of *d*. **a** Protein (4 μg) was incubated with (*lane 3*) or without (*lane 1*) 1 mM of DTT. *Lane 4*, subunit *d* was incubated with 100 μM $CuCl_2$ for 30 min before the addition of 1 mM DTT. *Lane 2*, *d* was supplemented with 100 μM $CuCl_2$ for 30 min. **b** Nonreduced subunit *d* was incubated with tetramethyl rhodamine (TMR, *lane1*) or N-ethyl maleimide (NEM, *lane 2*) for 30 min at 4°C before applying to an SDS-PAGE

of the mutant *d*C329S of the expected molecular mass in crude lysates following IPTG induction (Fig. 10b, lane 1) similar to the crude lysate of wild type subunit *d* cells (Fig. 10b, lane 2). However, the mutant protein was insoluble.

## Discussion

Subunit *d* of eukaryotic V-ATPases has been characterized as a nonintegrally associated $V_O$ subunit (Bauerle et al. 1993; Wang et al. 1988). Unlike other peripheral subunits, *d* remains stably associated with the membrane in the absence of the $V_1$ domain (Kane 1995; Sumner et al. 1995; Dames et al. 2006) and is not removed from the membrane portion by mild treatment with chaotropic agents (Bauerle et al. 1988, 1993; Kane et al. 1989; Wieczorek et al. 1999) or detergent ($C_{12}E_9$, Zhang et al. 1992). Only strong chaotropic agents or 5 M urea facilitate the detachment of the peripheral protein from the $V_O$ sector (Bauerle et al. 1993). In yeast, the loss of subunit *d* prohibits the remaining $V_O$ subunits from reaching the vacuole because of their inability to assemble and to form a $V_O$ subcomplex (Bauerle et al. 1993), and the $V_1$ particles are unable to associate with the membrane part, $V_O$ (Bauerle et al. 1993; Owegi et al. 2006). Most recently, the first data were described, implying that subunit *d* might be involved in coupling of proton transport and ATP hydrolysis (Nishi et al. 2003; Owegi et al. 2006). However, of the five eukaryotic $V_O$ subunits, the least characterized in terms of function and structure is subunit *d*. Like numerous other V-ATPase subunits in higher eukaryotes, subunit *d* appears to be encoded by multiple genes (Nishi et al. 2003; Miura et al. 2003, Merzendorfer et al. 2000; Smith et al. 2005; Sun-Wada et al. 2003) except in the case of yeast in which subunit *d* (Vma6p) is encoded by one gene, *Vma6*. The first isolation of the recombinant *d* (Vma6p) presented shows that this dehydrated protein, which because of its migration in electrophoresis experiments, has been called the 36 kDa protein (Bauerle et al. 1993), has a molecular weight of 40.1 kDa. The homogenous protein enabled us to get the first low resolution structure of the eukaryotic *d* in solution, showing a boxing glove-shaped molecule, consisting of two distinct domains (Fig. 6), a major part with a width of about 6.5 nm and a protuberance of about 3.5 nm in length. This structure is remarkably similar to the elongated mass located above the membrane-embedded $V_O$-domain of the cytoplasmic site of the bovine brain clathrin-coated vesicles, visualized in the 3D reconstruction and determined by single particle analysis of negatively stained electron micrographs (Wilkens and Forgac 2001, Fig. 11). According to the 3D-reconstruction this mass, predicted to belong to subunit *d*, seems to be directly linked to the cytosolic N-terminal part of subunit *a* of the $V_O$ domain (Wilkens and Forgac 2001). The structural comparison in Fig. 11 indicates that *d* is connected via its protuberance to the N-terminus of subunit *a*, and supports the association of both proteins as predicted from mutagenesis studies in which cells lacking *a*, the subunit *d* is not associated with the membrane, but found in the cytosol (Graham et al. 2000). As shown in the 3D reconstruction of the $V_O$ domain (Wilkens and Forgac 2001, and Fig. 11) the mass assigned now to subunit *d* is above and clearly lateral to the predicted ring, formed by the subunits $c_{4-5}$:$c'_1$:$c''_1$, and without any connection to it. The topology of subunit *d* inside the entire $V_1V_O$ ATPase is still a matter of debate. Mild proteolysis of the $V_1V_O$ ATPase in intact clathrin-coated vesicles resulted in rapid cleavage of *d*, suggesting that it is exposed inside the enzyme (Adachi et al. 1999). Since the N-terminus of subunit *a* becomes accessible for degradation in the absence of *d* (Hill and Coper 2000) and since the N-terminal part of *a* interacts directly with the catalytic A subunit (Landolt-Marticorena et al. 2000), whose N- and C-terminus are more than 18 nm and 6 nm above the membrane (Wilkens et al. 1999; Radermacher et al. 2001), respectively, models were described in which both, subunit *a* and *d* do form a peripheral stalk, thereby linking the $V_O$ sector with the $A_3B_3$-headpiece of the $V_1$ part (Clare et al. 2006; Forgac 2000). Like in the case of the peripheral stalk subunit *b* of the related $F_1F_O$ ATP synthase, laterally located cytoplasmic part of subunit *b* seen in the $F_O$-part (Singh et al. 1996) moves up after assembly with

**Table 1** MALDI-mass spectrometry analysis of peptides of subunit *d*, labeled with TMR and NEM, respectively, as well as the $CuCl_2$-and DTT-treated protein

| Subunit *d* | Start residue | End residue | Measured mass | Sequence |
|---|---|---|---|---|
| Non- | 1 | 18 | 2059.32 | MEGVYFNIDNGFIEGVVR |
| reduced | 19–43 | 322–335 | 4412.96 | $_{19}$GYRNGLLSNNQYINLTQCDTLELK$_{43}$[a] $_{322}$NITWIAECIAQNQR$_{335}$[a] |
| treated | 44 | 75 | 3443.72 | LQLSSTDYGNFLSSVSSESLTTSLIQEYASSK |
| with TMR | 85 | 93 | 964.99 | DQSSGSTRK |
| | 121 | 163 | 4850.65 | GEILQRCHPLGWFDTLPTLSVATDLESLYETVLVDTPLAPYFK |
| | 164 | 181 | 2625.35 | NCFDTAEELDDMNIEIIR[b] |
| | 206 | 218 | 1996.72 | ECMQTLLGFEADR[b] |
| | 206 | 219 | 2152.9 | ECMQTLLGFEADRR[b] |
| | 219 | 238 | 2053.26 | SINIALNSLQSSDIDPDLK |
| | 267 | 276 | 1169.30 | AALANVYEYR |
| | 277 | 297 | 3028.84 | GFLETGNLEDHFYQLEMELCR[b] |
| | 298 | 316 | 2245.58 | DAFTQQFAISTVWAWMKSK |
| $CuCl_2$- | 1 | 18 | 2059.32 | MEGVYFNIDNGFIEGVVR |
| treated | 22–43 | 322–335 | 4034.55 | $_{22}$NGLLSNNQYINLTQCDTLELK$_{43}$[a] $_{322}$NITWIAECIAQNQR$_{335}$[a] |
| | 44 | 75 | 3443.72 | LQLSSTDYGNFLSSVSSESLTTSLIQEYASSK |
| | 93 | 118 | 2954.42 | FMDYITYGYMIDNVALMITGTIHDR |
| | 121 | 181 | 6971.90 | GEILQRCHPLGWFDTLPTLSVATDLESLYETVLVDTPLAPYFKNCFD TAEELDDMNIEIIR[a] |
| | 206 | 218 | 1510.72 | ECMQTLLGFEADR |
| | 206 | 218 | 1666.90 | ECMQTLLGFEADRR |
| | 219 | 238 | 2053.26 | SINIALNSLQSSDIDPDLK |
| | 248 | 266 | 2176.46 | LYPLATFHLAQAQDFEGVR |
| | 267 | 297 | 3696.12 | AALANVYEYRGFLETGNLEDHFYQLEMELCR |
| | 298 | 314 | 2030.33 | DAFTQQFAISTVWAWMK |
| DTT- | 1 | 18 | 2059.32 | MEGVYFNIDNGFIEGVVR |
| treated | 22 | 43 | 2394.68 | NGLLSNNQYINLTQCDTLELK |
| | 44 | 75 | 3443.72 | LQLSSTDYGNFLSSVSSESLTTSLIQEYASSK |
| | 85 | 93 | 964.99 | DQSSGSTRK |
| | 92 | 120 | 3325.86 | KFMDYITYGYMIDNVALMITGTIHDRDK |
| | 121 | 163 | 4850.56 | GEILQRCHPLGWFDTLPTLSVATDLESLYETVLVDTPLAPYFK |
| | 164 | 181 | 2141.35 | NCFDTAEELDDMNIEIIR |
| | 187 | 205 | 2275.50 | AYLEDFYNFVTEEIPEPAK |
| | 206 | 238 | 3694.15 | ECMQTLLGFEADRRSINIALNSLQSSDIDPDLK |
| | 248 | 266 | 2176.46 | LYPLATFHLAQAQDFEGVR |
| | 317 | 335 | 2301.56 | EQEVRNITWIAECIAQNQR |
| | 322 | 335 | 1659.88 | NITWIAECIAQNQR |
| Non- | 1 | 18 | 2059.32 | MEGVYFNIDNGFIEGVVR |
| reduced | 19–43 | 322–355 | 4412.96 | $_{19}$GYRNGLLSNNQYINLTQCDTLELK$_{43}$[a] $_{322}$NITWIAECIAQNQR$_{335}$[a] |
| treated | 44 | 75 | 3443.72 | LQLSSTDYGNFLSSVSSESLTTSLIQEYASSK |
| with NEM | 121 | 163 | 4489.87 | GEILQRCHPLGWFDTLPTLSVATDLESLYETVLVDTPLAPYFK[c] |
| | 164 | 181 | 2264.55 | NCFDTAEELDDMNIEIIR[c] |
| | 206 | 218 | 1635.94 | ECMQTLLGFEADR[c] |
| | 206 | 219 | 1792.12 | ECMQTLLGFEADRR[c] |
| | 219 | 238 | 2053.26 | SINIALNSLQSSDIDPDLK |
| | 267 | 276 | 1169.30 | AALANVYEYR |
| | 277 | 297 | 2668.06 | GFLETGNLEDHFYQLEMELCR[c1] |

[a] Peptides involved in disulfide formation via Cys residues.
[b] Peptides labeled with TMR.
[c] Peptides labeled with NEM

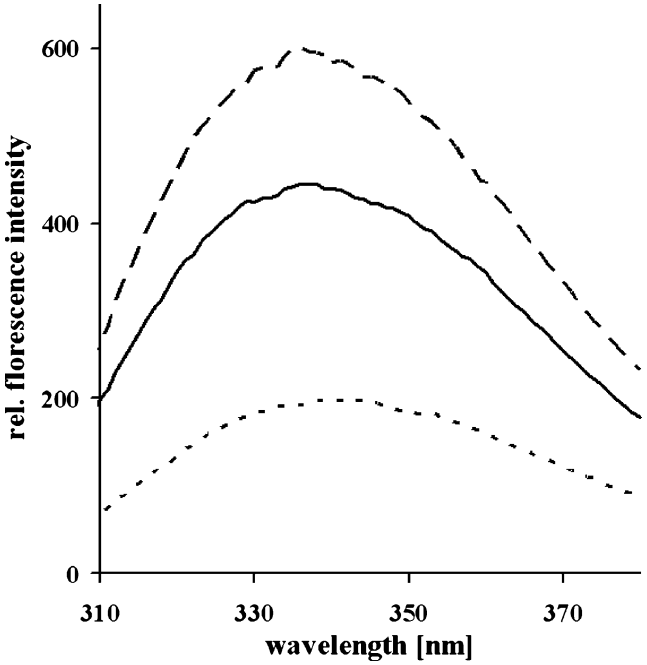


**Fig. 9** The tryptophan fluorescence emission spectra of subunit *d*. (—) nonreduced protein; (- -) *d* after reduction by 1 mM of DTT; (· ·) subunit *d* supplemented with 100 μM $CuCl_2$ for 30 min. Excitation was at 295 nm with excitation and emission bandpasses set to 5 nm

the $F_1$ sector, connecting the membrane-embedded $F_O$ with the N-terminal part of the $\alpha_3\beta_3$-headpiece of the $F_1$ section (Wilkens and Capaldi 1998). Taking this into account the cavity of the boxing glove-shaped *d* may enable the elongated assembly of the *a–d* domain to bind to the exposed non-homologous region of the catalytic A, which is linked to both coupling of proton transport and ATP hydrolysis and dissociation of the $V_1V_O$ ATPase complex in vivo (Fig. 1; Shao et al. 2003). Furthermore, the extended assembly of *a* and *d* would provide the surface for the interaction of *a* with the elongated GDP/GTP exchange factor ARNO (ADP-ribosylation factor nucleotide site opener) with a mass of about 50 kDa (Frank et al. 1998), and at the same time making the $V_O$-ring, formed by subunit c, accessible for its assembly with the GTPase Arf6. Such an interaction of the V-ATPase with ARNO and Arf6 has recently been found in early endosomes, regulating the protein degradation pathways (Hurtado-Lorenzo et al. 2006).

Vma6p (subunit *d*) as isolated, is highly helical with a significant degree of helix–helix interaction based on the $\Theta_{222}/\Theta_{208}$ ratio of about 1.0. Subunit *d* from all species of eukaryotic V-ATPases shows a very high degree of sequence identity and homology, going along with two and one conserved cysteine residues in the N- ($Cys_{36,127}$) and C-terminus ($Cys_{329}$), respectively (Fig. 7). The disulphide bond formed by $Cys_{36}$ and $Cys_{329}$, bridging peptides $_{19}$GYRNGLLSNNQYINLTQCDTLELK$_{43}$ and $_{322}$NITWIAECIAQNQR$_{335}$, demonstrate the near neighborhood of both termini and are an example of helix–helix interaction inside the protein as discussed above. In this context it is of interest that the truncated forms $d_{1–328}$,

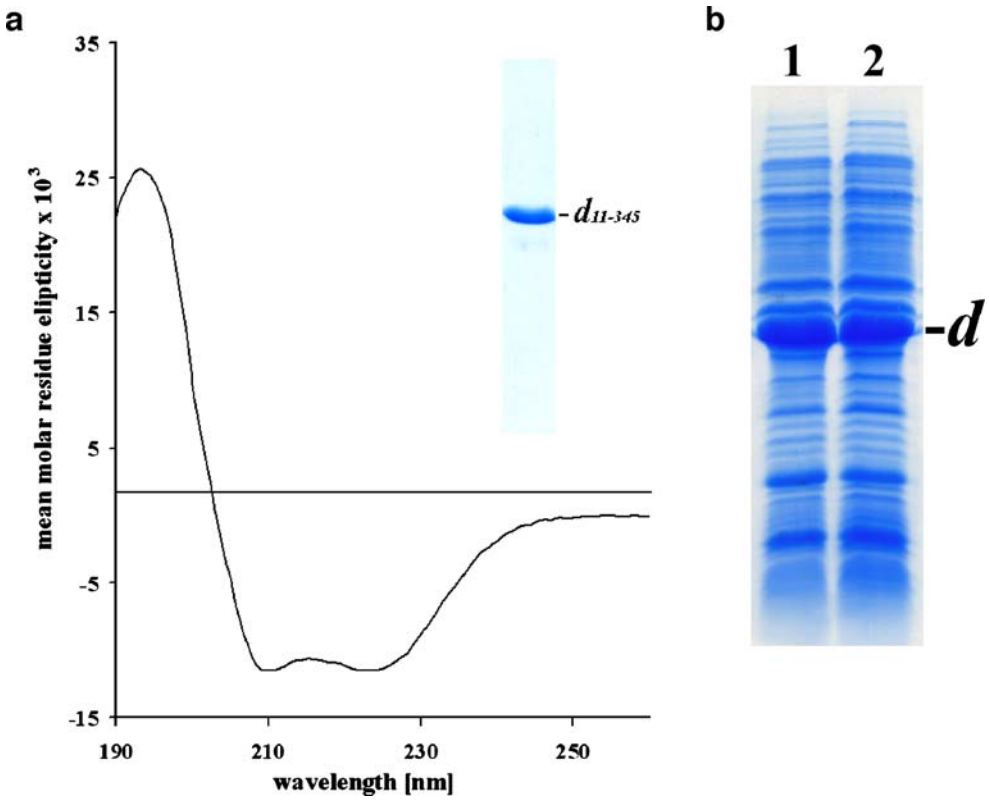


**Fig. 10** **a** Far UV-CD spectrum of the truncated form $d_{11–345}$. (*Insert*), SDS-gel shows a sample of the recombinant $d_{11–345}$ protein used in the CD spectroscopy measurement. **b** SDS-PAGE (17.5% total acrylamide and 0.4% cross-linked acrylamide gel) of *E. coli* lysates showing the produced mutant protein *d*C329S (*lane 1*) and subunit *d* (*lane 2*)

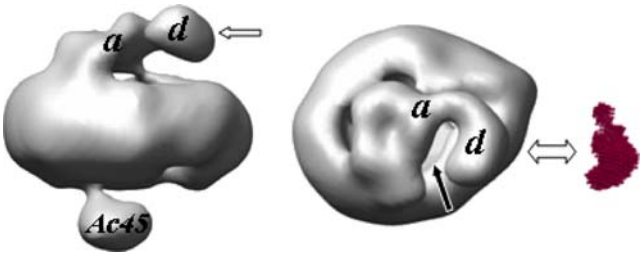


**Fig. 11** Shape comparison of the low resolution structure of subunit *d* (*red*) from yeast in solution with the predicted position of subunit *d* inside the three-dimensional reconstruction of the $V_O$ domain from bovine brain clathrin-coated vesicles, derived from single particle analysis of electron micrographs (Wilkens and Forgac 2001). Subunit *a* and Ac45 are located according to the topological model of the V-ATPase from yeast (Wilkens et al. 1999) and clathrin-coated vesicles (Wilkens and Forgac 2001). The *black arrow* indicates the cytoplasmic opening of the channel

$d_{1–298}$ and $d_{38–345}$, lacking either of the two conserved Cys residues ($Cys_{36}$ and $Cys_{329}$), and the point mutant *d*C329S, lead to less and/or insoluble proteins, whereby $d_{11–345}$ was expressed as a soluble and properly folded protein, comparable to the entire subunit *d*. The addition of excess of DTT resulted in the reduction of the Cys–Cys bond, and slight changes of the secondary structure as detected by CD and intrinsic tryptophan fluorescence spectroscopy. These data reflect that the disulphide formation seems to be essential in the process of protein folding rather than stabilization of the produced subunit. In case of the protein folding pathway of subunit *d* in *S. cerevisiae* the process of thiol–disulfide interchange reaction would be catalyzed by the chaperone protein disulfide isomerase, which is essential for the oxidation of thiols, the reduction and isomerization (Woycechowsky and Raines 2000; Yano et al. 2002). The described importance of both termini in protein folding is in line with transformations of N- and C-truncated forms of Vma6p into yeast cells, showing slow or no growth, and a drop of 60% of ATPase activity of vacuolar membranes from the mutant *d*C329A (Owegi et al. 2006). Importance of protein folding during the production in *E. coli* is further supported by the fact that a substantial increase in the production and solubility was observed in Rosetta-gammi 2 cells, which facilitate enhanced disulphide formation and/or folding of protein compared to BL21 DE3, which lacks such machinery.$CuCl_2$-treatment of subunit *d* results in an additional disulphide bond, formed between $Cys_{127}$ and $Cys_{165}$, and indicating their close proximity. The structural alterations detected by CD and fluorescence spectroscopy, and the migration of the protein in gel electrophoresis seems to alter the secondary—rather than the tertiary structure, as shown by SAXS experiments. MALDI-TOF analysis of the non-reduced and $CuCl_2$ crosslinked *d* also revealed that $Cys_{127}$ is accessible for NEM but not for the more bulky fluorophore TMR and therefore is not exposed in the protein like the labeled residues $Cys_{165}$, $Cys_{207}$ and $Cys_{296}$.

Although subunit C of the bacterial $A_1A_O/V_1V_O$ ATP synthase shows rather low (18%) sequence homology (Owegi et al. 2006; Iwata et al. 2004), and no conserved cysteine residue pattern (Iwata et al. 2004), subunit *d* of the eukaryotic V-ATPases have been predicted to be similar in structure and function (Yokoyama and Imamura 2005). (Note, the so-called $V_1V_O$ ATPase from both *Thermus thermophilus* and *Enterococcus hirae*, which primarily synthesize ATP, are of archaeal origin translocated by horizontal gene transfer (Bernal and Stock 2004; Olendzenski et al. 1998) and will be considered as $A_1A_O/V_1V_O$ ATP synthases during this publication.). The distance distribution function computed from the scattering pattern from the atomic model of the *T. thermophilus* C subunit (Iwata et al. 2004) displays that the structures of both subunits differ significantly. The symmetric profile of the distance distribution function (Fig. 5b) characterizes the more compact structure of subunit C with a funnel shape (Iwata et al. 2004). The major differences in the tertiary structure of subunit C of the bacterial $A_1A_O/V_1V_O$ ATP synthase (Iwata et al. 2004) and subunit *d* of the eukaryotic $V_1V_O$ ATPase are that *d* is not only larger but also more anisometric, reflected by its boxing glove-shape. Superposition of the crystal structure of subunit C (Iwata et al. 2004) and the low resolution structure of *d* presented, indicates also the differences in the additional volume of the upper- and the protuberance of the lower part present in subunit *d* (Fig. 6d). Whereas subunit *d* of V-ATPases is strongly attached to the Vo section during the physiological process of reversible disassembly of the $V_1V_O$ ATPase (Kane 1995; Sumner et al. 1995; Dames et al. 2006) and even during treatment with chaotropic agents (Bauerle et al. 1993; Kane et al. 1989; Wieczorek et al. 1999), subunit C of most $A_1A_O/V_1V_O$ ATP synthase are linked to the $A_1/V_1$ domain (Chaban et al. 2002; Kakinuma et al. 1999; Coskun et al. 2004), thereby forming the bottom of the central stalk, and functionally linking the catalytic site events in the $A_3B_3$ hexamer with ion-conduction in the membrane section visa-versa (Chaban et al. 2002; Coskun et al. 2004, Grüber et al. 2000). These structural, biochemical and topological diversities of both proteins are in line with the fact that subunit C of the *T. thermophilus* $A_1A_O/V_1V_O$ ATP synthase does not functionally substitute for subunit *d* and does not complement the phenotype of *vma6*Δ cells as shown most recently (Owegi et al. 2006).

In summary, the data presented demonstrate that subunit *d* (Vma6p) of the yeast vacuolar ATPase exists in solution as an elongated molecule, organized as two well-defined domains, as determined by two ab initio shape restoration procedures. The similarity in shape with the mass of the recently determined 3D-reconstrution of the $V_O$ domain (Wilkens and Forgac 2001) allows for the first time a clear assignment of subunit *d* inside the membrane part, $V_O$. The

proper folding of this protein becomes facilitated due to a disulphide bond formation of the $Cys_{36}$ and $Cys_{329}$, located in the N- and C-terminus of Vma6p, respectively. Because of its strong interaction with subunit *a*, the findings about Vma6p presented might give new implication about an involvement of subunit *d* in regulation of the reversible $V_1V_O$ disassembly and ATP hydrolysis driven proton conduction.

**Acknowledgment** We are grateful to Prof. S. Wilkens (Upstate Medical University, New York, USA) for providing us the 3D reconstruction images of the $V_O$ domain. S. Gayen and Dr. S. Vivekanandan are acknowledged for help with NMR data collection at the School of Biological Sciences (SBS), Nanyang Technological University (NTU), Singapore. We thank Dr. A. Grüber (SBS) for her support in MALDI-TOF data analysis. Y. R. Thaker is a recipient of the Graduate Research Scholarship, School of Biological Sciences (SBS), Nanyang Technological University (NTU), Singapore. This research was supported by the SBS, NTU, Singapore (SBS/SUG/31/05).

## References

Adachi I, Puopolo K, Marquez-Sterling N, Arai H, Forgac M (1999) J Biol Chem 265:967–973
Bauerle C, Magembe C, Briskin DP (1988) Plant Physioliol 117:859–867
Bauerle C, Ho MN, Lindorfer MA, Stevens TH (1993) J Biol Chem 268:12749–12757
Bernal RA, Stock D (2004) Structure 12:1789–1798
Bernstein FC, Koetzle TF, Williams GJB, Meyer EG Jr, Brice MD, Rodgers JR, Kennard O, Shimanouchi T, Tasumi M (1977) J Mol Biol 112:535–542
Boulin CJ, Kempf R, Koch MHJ, McLaughlin SM (1986) Nucl Instrum Methods, A 249:399–407
Boulin CJ, Kempf R, Gabriel A, Koch MHJ (1988) Nucl Instrum Methods, A 269:312–320
Burkhard P, Stetefeld J, Streikov SV (2001) Trends Cell Biol 11:82–88
Chaban Y, Ubbink-Kok T, Keegstra W, Lolkema JS, Boekema EJ (2002) EMBO Rep 3:1–10
Clare DK, Orlova EV, Finbow MA, Harrison MA, Findlay JB, Saibil HR (2006) Structure 14:1149–1156
Coskun Ü, Radermacher M, Müller V, Ruiz T, Grüber G (2004) J Biol Chem 279:22759–22764
Dames P, Zimmermann B, Schmidt R, Rein J, Voss M, Schewe B, Walz B, Baumann O (2006) Proc Natl Acad Sci USA 103:3926–3931
Forgac M (2000) J Exp Biol 203:71–80
Frank S, Upender S, Hansen SH, Casanova JE (1998) J Biol Chem 273:23–27
Graham LA, Powell B, Stevens TH (2000) J Exp Biol 203:61–70
Grüber G, Svergun DI, Coskun Ü, Lemker T, Koch MHJ, Schägger H, Müller V (2000) Biochemistry 40:1890–1896
Guinier A, Fournet G (1955) Small-angle scattering of X-rays. Wiley, New York
Hill K, Coper AA (2000) EMBO J 19:550–561
Hurtado-Lorenzo A, Skinner M, Annan JE, Futai M, Sun-Wada G-H, Bourgoin S, Casanova J, Wildeman A, Bechoua S, Ausiello DA, Brown D, Marshansky V (2006) Nat Cell Biol 8:124–136
Inoue T, Wilkens S, Forgac M (2003) J Bioenerg Biomembranes 35:291–300
Iwata M, Imamura H, Stambouli E, Ikeda C, Tamakoshi M, Nagata K, Makyio H, Hankamer B, Barber J, Yoshida M, Yokoyama K, Iwata S (2004) Proc Natl Acad Sci USA 101:59–64
Kakinuma Y, Yamato I, Murata T (1999) J Bioenerg Biomembranes 31:7–14
Kane PM (1995) J Biol Chem 270:17025–17032
Kane PM, Yamashiro CT, Stevens TH (1989) J Biol Chem 264:19236–19244
Konarev PV, Volkov V, Sokolova AV, Koch MHJ, Svergun DI (2003) J Appl Crystallogr 36:1277–1282
Laemmli UK (1970) Nature 227:680–685
Landolt-Marticorena C, Williams KM, Correa J, Chen W, Manolson MF (2000) J Biol Chem 275:15449–15457
Lolkema JS, Chaban Y, Boekema EJ (2003) J Bioenerg Biomembranes 35:323–336
Margolles-Clark E, Tenney K, Bowman EJ, Bowman BJ (1999) J Bioenerg Biomembranes 31:29–37
Melnik VI, Bowman BJ (1996) Biochim Biophys Acta 1273:77–83
Merzendorfer H, Harvey WR, Wieczorek H (1997) FEBS Lett 411:239–244
Merzendorfer H, Reineke S, Zhao X-F, Jacobmeier B, Harvey WR, Wieczorek H (2000) Biochim Biophys Acta 1467:369–379
Mezghrani A, Fassio A, Benham A, Simmen T, Braakman I, Sitia R (2001) EMBO J 20:6288–6296
Miura GI, Froelick GJ, Marsh DJ, Stark KL, Palmiter RD (2003) Transgenic Res 12:131–133
Müller V, Grüber G (2003) Cell Mol Life Sci 60:474–494
Nishi T, Kawasaki-Nishi S, Forgac M (2003) J Biol Chem 278:46396–46402
Olendzenski L, Hilario E, Gogarten JP (1998) In: Syvanen K, Kado CI (eds) Horizontal gene transfer. Chapman & Hall, New York, pp 349–362
Owegi MA, Pappas DL, Finch MW Jr, Bilbo SA, Resendiz CA, Jacquemin LJ, Warrier A, Trombley JD, McCulloch KM, Margalef KLM, Mertz MJ, Storms JM, Damin CA, Parra KJ (2006) J Biol Chem 281:30001–30014
Page R, Peti W, Wilson IA, Stevens RC, Wüthrich K (2005) Proc Natl Acad Sci USA 102:1901–1905
Radermacher M, Ruiz T, Wieczorek H, Grüber G (2001) J Struct Biol 135:26–37
Roos M, Soskic V, Poznanovic S, Godovac-Zimmermann J (1998) J Biol Chem 273:924–931
Shao E, Nisji T, Kawasaki-Nishi S, Forgac M (2003) J Biol Chem 278:12985–12991
Singh S, Turina P, Bustamante CJ, Keller DJ, Capaldi RA (1996) FEBS Lett 397:30–34
Smith AN, Jouret F, Bord S, Borthwick KJ, Al-Lamki RS, Wagner CA, Ireland DC, Cormier-Daire V, Frattini A, Villa A, Kornak U, Devuyst O, Karet FE (2005) J Am Soc Nephrol 16:1245–1256
Sumner JP, Dow JAT, Earley FG, Klein U, Jäger D, Wieczorek H (1995) J Biol Chem 270:5649–5653
Sun-Wada G-H, Soshimizu T, Imai-Senga Y, Wada Y, Futai M (2003) Gene 302:147–153
Svergun DI (1992) J Appl Crystallogr 25:495–503
Svergun DI (1993) J Appl Crystallogr 26:258–267
Svergun DI (1997) J Appl Crystallogr 30:792–797
Svergun DI, Barberato C, Koch MHJ (1995) J Appl Crystallogr 28:768–773
Svergun DI, Beæireviæ A, Schrempf H, Koch MHJ, Grüber G (2000) Biochemistry 39:10677–10683
Svergun DI, Petoukhov MV, Koch MHJ (2001) Biophys J 80:2946–2953
Temesvari L, Rodriguez, Paris J, Bush J, Steck TL, Cardelli J (1994) J Biol Chem 269:25719–25727
Venzke D, Domgall I, Köcher T, Féthière J, Fischer S, Böttcher B (2005) J Mol Biol 349:659–669

Wang SY, Moriyama Y, Mandel M, Hulmes JD, Pan YC, Danho W, Nelson H, Nelson N (1988) J Biol Chem 263:17638–17642
Wieczorek H, Grüber G, Harvey WR, Huss M, Merzendorfer H (1999) J Bioenerg Biomembranes 31:67–74
Wilkens S, Capaldi RA (1998) Biochim Biophys Acta 1365:93–97
Wilkens S, Forgac M (2001) J Biol Chem 276:44064–44068
Wilkins MR, Lindskog I, Gasteiger E, Bairoch A, Sanchez JC, Hochstrasser DF, Appel RD (1997) Electrophoresis 18:403–408
Wilkens S, Vasilyeva E, Forgac M (1999) J Biol Chem 274:31804–31810
Woycechowsky KJ, Raines RT (2000) Curr Opin Chem Biol 4:533–539
Yano H, Kuroda S, Buchanan BB (2002) Proteomics 2:1090–1096
Yokoyama K, Imamura H (2005) J Bioenerg Biomembranes 37:405–410
Zhang J, Myers M, Forgac M (1992) J Biol Chem 267:9773–97784